

A Geometric Perspective on Diffusion Models

Yuanzhi Zhu

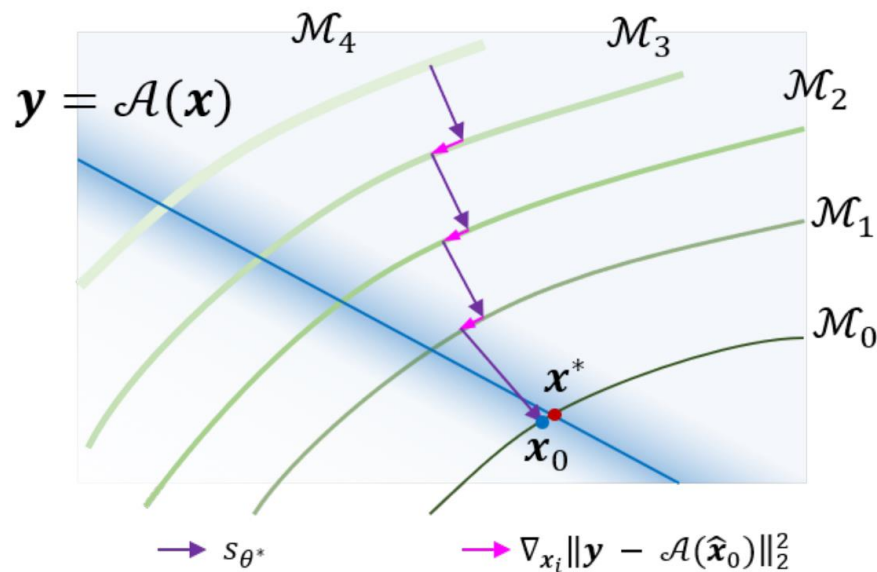
Content

- Motivation
- Geometric Perspective
- Conclusion

A Geometric Perspective on Diffusion Models*

(my) Motivation: Not related to non-Euclidean geometry

1. How to understand this graph?



A Geometric Perspective on Diffusion Models

(my) Motivation: Not related to MOLECULAR generation

2. What's the difference between the following two algorithm?

Algorithm 1 DiffPIR

Require: $s_\theta, T, \mathbf{y}, \sigma_n, \{\bar{\sigma}_t\}_{t=1}^T, \zeta, \lambda$

- 1: Initialize $\mathbf{x}_T \sim \mathcal{N}(\mathbf{0}, \mathbf{I})$, pre-calculate $\rho_t \triangleq \lambda \sigma_n^2 / \bar{\sigma}_t^2$.
 - 2: **for** $t = T$ **to** 1 **do**
 - 3: $\mathbf{x}_0^{(t)} = \frac{1}{\sqrt{\bar{\alpha}_t}}(\mathbf{x}_t + (1 - \bar{\alpha}_t)s_\theta(\mathbf{x}_t, t))$ // Predict $\hat{\mathbf{z}}_0$ with score model as denoisor
 - 4: $\hat{\mathbf{x}}_0^{(t)} = \arg \min_{\mathbf{x}} \|\mathbf{y} - \mathcal{H}(\mathbf{x})\|^2 + \rho_t \|\mathbf{x} - \mathbf{x}_0^{(t)}\|^2$ // Solving data proximal subproblem
 - 5: $\hat{\epsilon} = \frac{1}{\sqrt{1 - \bar{\alpha}_t}}(\mathbf{x}_t - \sqrt{\bar{\alpha}_t} \hat{\mathbf{x}}_0^{(t)})$ // Calculate effective $\hat{\epsilon}(\mathbf{x}_t, \mathbf{y})$
 - 6: $\epsilon_t \sim \mathcal{N}(\mathbf{0}, \mathbf{I})$
 - 7: $\mathbf{x}_{t-1} = \sqrt{\bar{\alpha}_{t-1}} \hat{\mathbf{x}}_0^{(t)} + \sqrt{1 - \bar{\alpha}_{t-1}}(\sqrt{1 - \zeta} \hat{\epsilon} + \sqrt{\zeta} \epsilon_t)$ // Finish one step reverse diffusion sampling
 - 8: **end for**
 - 9: **return** \mathbf{x}_0
-

Algorithm 2 Extended Sampling I: DPS y_t

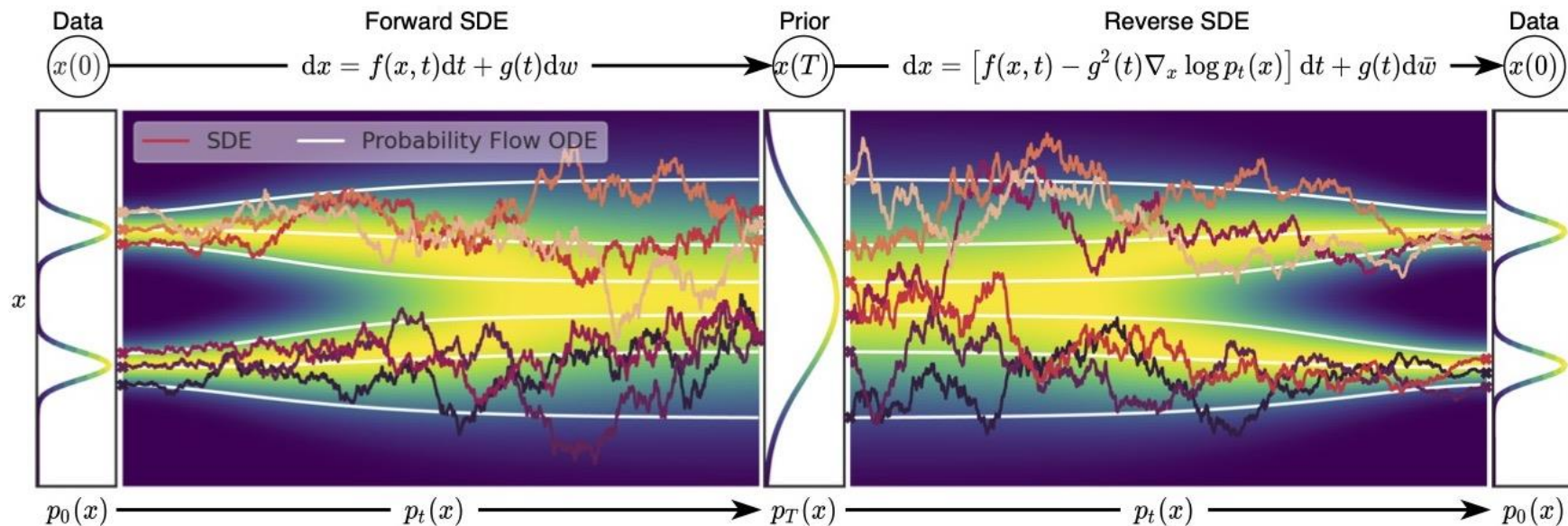
Require: $s_\theta, T, \mathbf{y}, \sigma_n, \{\sigma_t\}_{t=1}^T, \lambda$

- 1: Initialize $\mathbf{x}_T \sim \mathcal{N}(\mathbf{0}, \mathbf{I})$
 - 2: **for** $t = T$ **to** 1 **do**
 - 3: $\epsilon_t \sim \mathcal{N}(\mathbf{0}, \mathbf{I})$
 - 4: $\mathbf{z}_{t-1} = \frac{1}{\sqrt{\alpha_t}} \left(\mathbf{x}_t - \frac{\beta_t}{\sqrt{1 - \bar{\alpha}_t}} \epsilon_\theta(\mathbf{x}_t, t) \right) + \sqrt{\beta_t} \epsilon_t$ // one step reverse diffusion sampling
 - 5: $\mathbf{x}_{t-1} = \mathbf{z}_{t-1} - \frac{\sigma_t^2}{2\lambda\sigma_n^2} \nabla_{\mathbf{z}_{t-1}} \|\mathbf{y}_{t-1} - \mathcal{H}(\mathbf{z}_{t-1})\|^2$ // Solving data proximal subproblem
 - 6: **end for**
 - 7: **return** \mathbf{x}_0
-

A Geometric Perspective on Diffusion Models

(my) Motivation: Use only VE-ODE for example

3. How to understand the diffusion trajectory better?



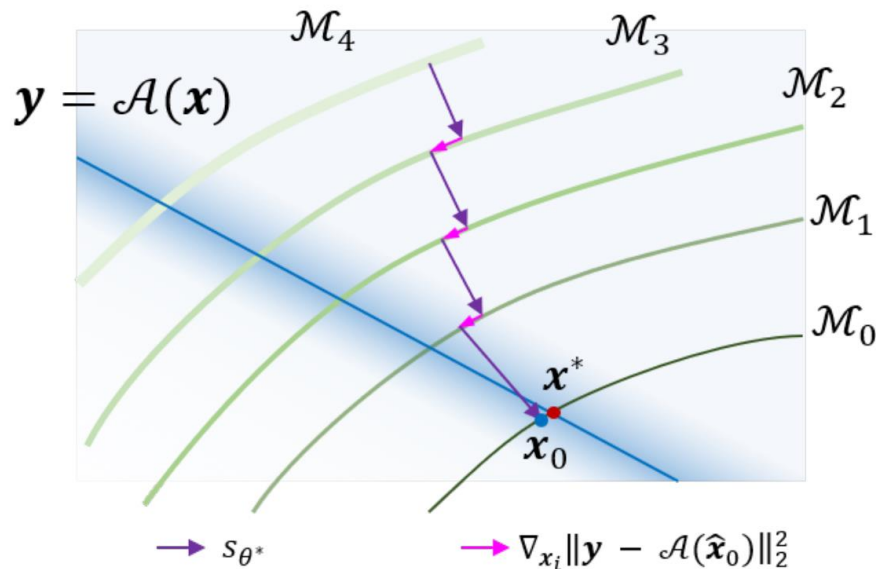
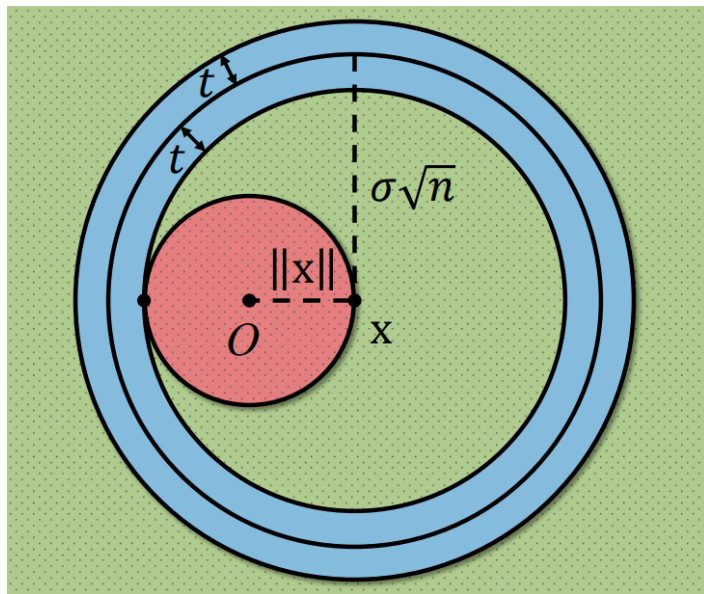
Content

- Motivation
- Geometric Perspective
- Conclusion

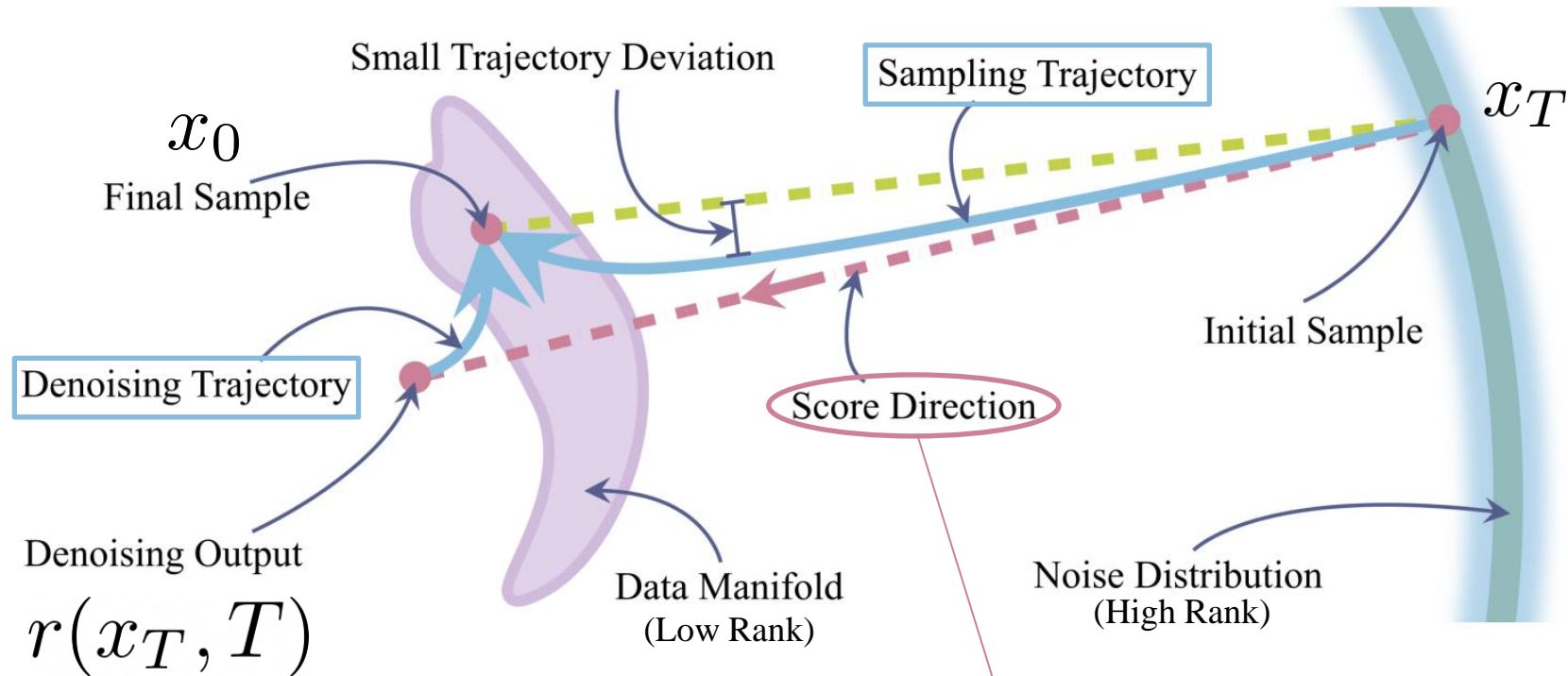
Visualization of High Dimensional Trajectory

Proposition 1. Given a high-dimensional vector $\mathbf{x} \in \mathbb{R}^d$ and an isotropic Gaussian noise $\mathbf{z} \sim \mathcal{N}(\mathbf{0}; \sigma^2 \mathbf{I}_d)$, $\sigma > 0$, we have $\mathbb{E} \|\mathbf{z}\|^2 = \sigma^2 d$, and with high probability, \mathbf{z} stays within a “thin shell”:
 $\|\mathbf{z}\| = \sigma\sqrt{d} \pm O(1)$. Additionally, $\mathbb{E} [\|\mathbf{x} + \mathbf{z}\|^2 - \|\mathbf{x}\|^2] = \sigma^2 d$, $\lim_{d \rightarrow \infty} \mathbb{P}(\|\mathbf{x} + \mathbf{z}\| > \|\mathbf{x}\|) = 1$.

Perpendicular



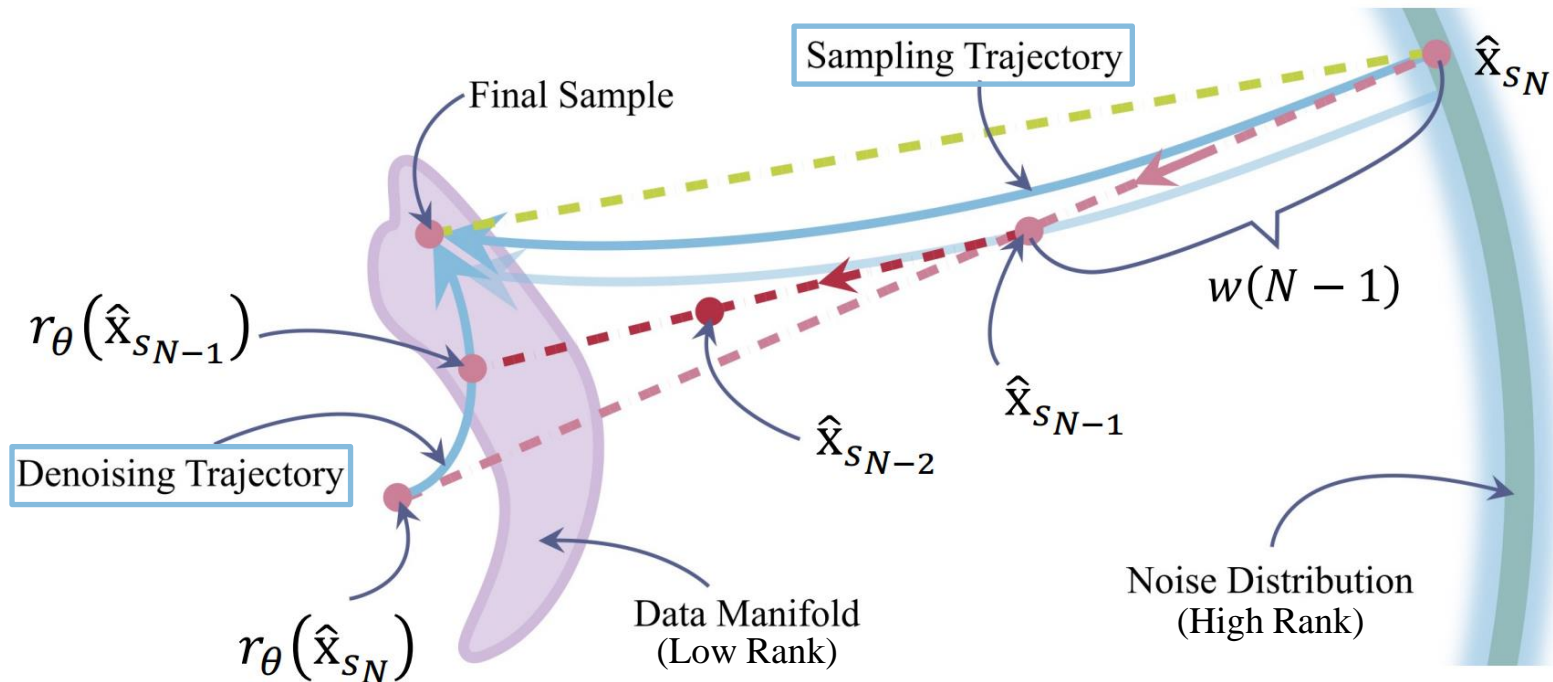
Visualization of High Dimensional Trajectory



$$\frac{dx}{dt} = -\dot{\sigma}(t)\sigma(t)\nabla \log p(x, \sigma(t)) = -\dot{\sigma}(t) \frac{r(x, \sigma(t)) - x}{\sigma(t)} \xrightarrow{\sigma(t)=t} -\frac{r(x, t) - x}{t}$$

Visualization of High Dimensional Trajectory

1. Straightness of the trajectories
2. Properties of denoising trajectory



Experiments on High Dimensional Trajectory

Notations:

sampling trajectory sequence $\{\hat{\mathbf{x}}_s\}_{s_N}^{s_0}$ (reverse diffusion with trained model)

optimal sampling sequence $\{\hat{\mathbf{x}}_s^*\}_{s_N}^{s_0}$ (forward diffusion of image from dataset)

ℓ_2 distance $d(\cdot, \cdot)$

trajectory deviation $d(\hat{\mathbf{x}}_s, [\hat{\mathbf{x}}_{s_0}, \hat{\mathbf{x}}_{s_N}])$ (straightness)

denoising trajectory sequence $\{r_\theta(\hat{\mathbf{x}}_s, s)\}_{s_N}^{s_1}$

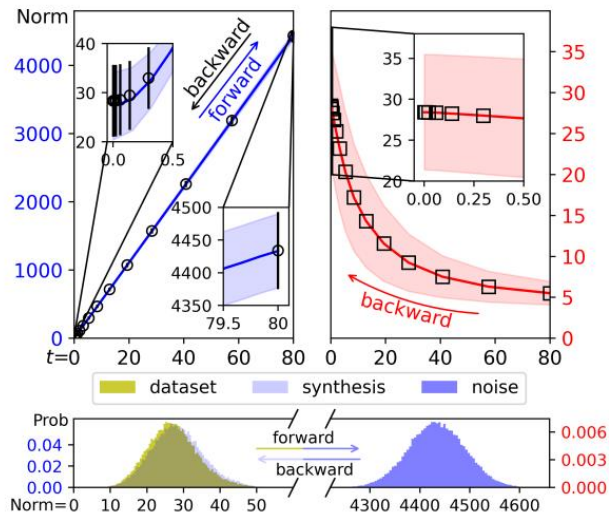
optimal denoiser

$$r_{\theta}^*(\hat{\mathbf{x}}; \sigma_t) = \sum_i u_i \mathbf{x}_i = \sum_i \frac{\exp(-\|\hat{\mathbf{x}} - \mathbf{x}_i\|^2 / 2\sigma_t^2)}{\sum_j \exp(-\|\hat{\mathbf{x}} - \mathbf{x}_j\|^2 / 2\sigma_t^2)} \mathbf{x}_i, \quad \sum_i u_i = 1.$$

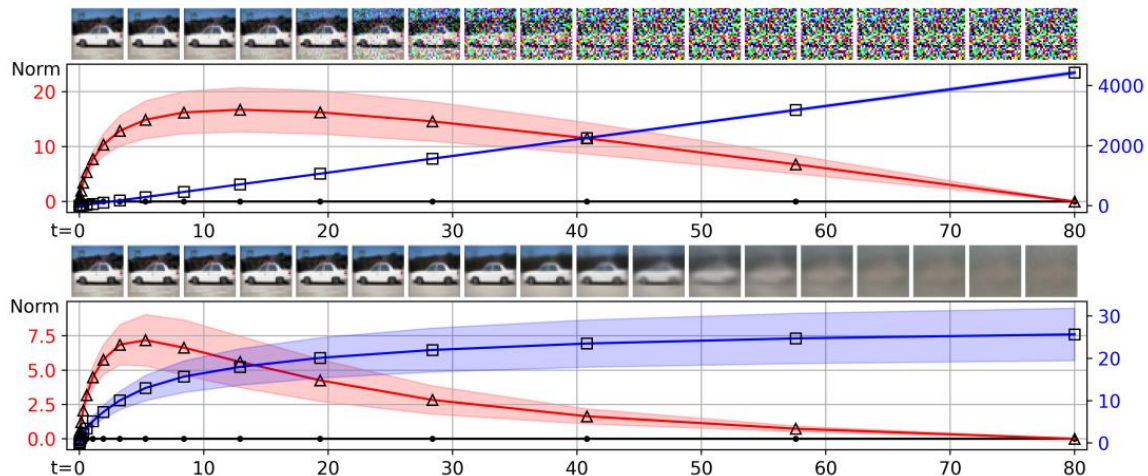
Experiments on High Dimensional Trajectory

Observation 1. The sampling trajectory is almost straight while the denoising trajectory is bent.

Observation 2. The generated samples on the sampling trajectory and denoising trajectory both move monotonically from the initial points toward their converged points in expectation, i.e., $\{\mathbb{E}[d(\hat{\mathbf{x}}_s, \hat{\mathbf{x}}_{s_0})]\}_{s_N}^{s_0}$ and $\{\mathbb{E}[d(r_\theta(\hat{\mathbf{x}}_s), r_\theta(\hat{\mathbf{x}}_{s_1}))]\}_{s_N}^{s_1}$ are monotone decreasing sequences.



(a) The statistics of magnitude.



(b) Deviation in the sampling (top)/denoising (bottom) trajectories.

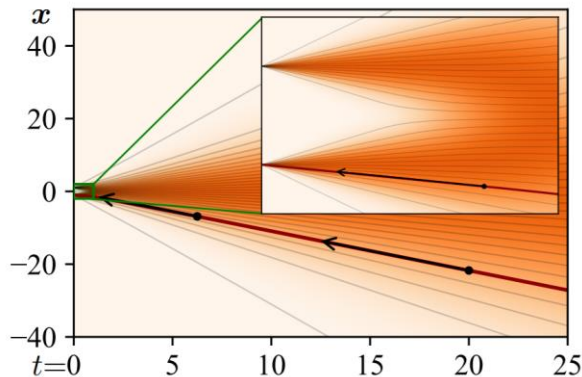
Experiments on High Dimensional Trajectory

Observation 3. *The sampling trajectory converges to the data distribution in a monotone magnitude shrinking way. Conversely, the denoising trajectory converges to the data distribution in a monotone magnitude expanding way. Formally, we have $\{\mathbb{E}\|\hat{\mathbf{x}}_s\|\}_{s_N}^{s_0} \downarrow$ and $\{\mathbb{E}\|r_\theta(\hat{\mathbf{x}}_s)\|\}_{s_N}^{s_1} \uparrow$.*

optimal denoiser:
$$r_\theta^*(\hat{\mathbf{x}}; \sigma_t) = \sum_i u_i \mathbf{x}_i = \sum_i \frac{\exp(-\|\hat{\mathbf{x}} - \mathbf{x}_i\|^2 / 2\sigma_t^2)}{\sum_j \exp(-\|\hat{\mathbf{x}} - \mathbf{x}_j\|^2 / 2\sigma_t^2)} \mathbf{x}_i, \quad \sum_i u_i = 1.$$

1D example with two source data point (-1) and (+1) (from [EDM](#))

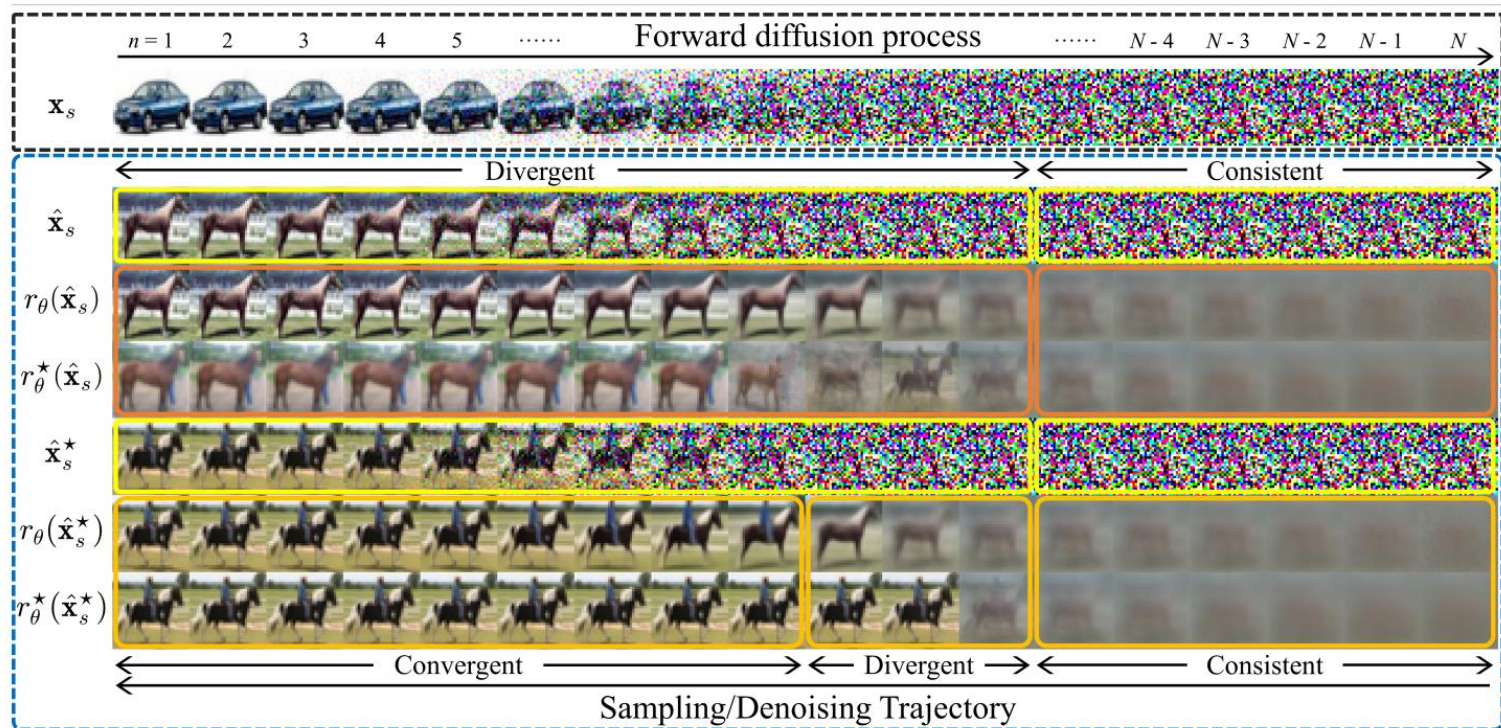
$$r_\theta^*(\hat{\mathbf{x}}; \sigma_t) \xrightarrow{\sigma_t \rightarrow \infty} \mathbb{E}[\mathbf{x}_i]$$



$$\frac{dx}{dt} = -\frac{r(x, t) - x}{t}$$

(c) DDIM [47] / Our ODE

Experiments on High Dimensional Trajectory



Experiments on High Dimensional Trajectory

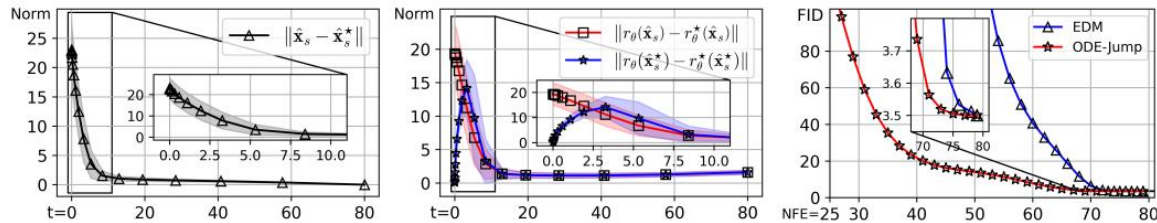
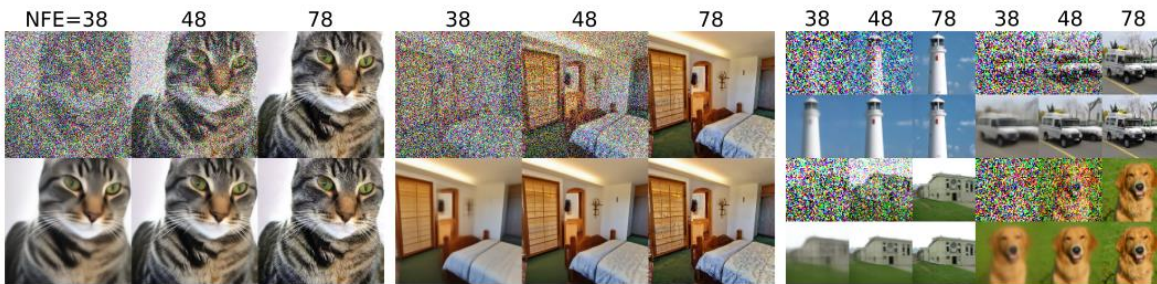


Figure 4: The score deviation in expectation (left and middle) and FID with different NFEs (right).

Observation 4. *The learned score is well-matched to the optimal score in the large-noise region (from 80 to around 10), otherwise they may diverge or almost coincide depending on different regions*



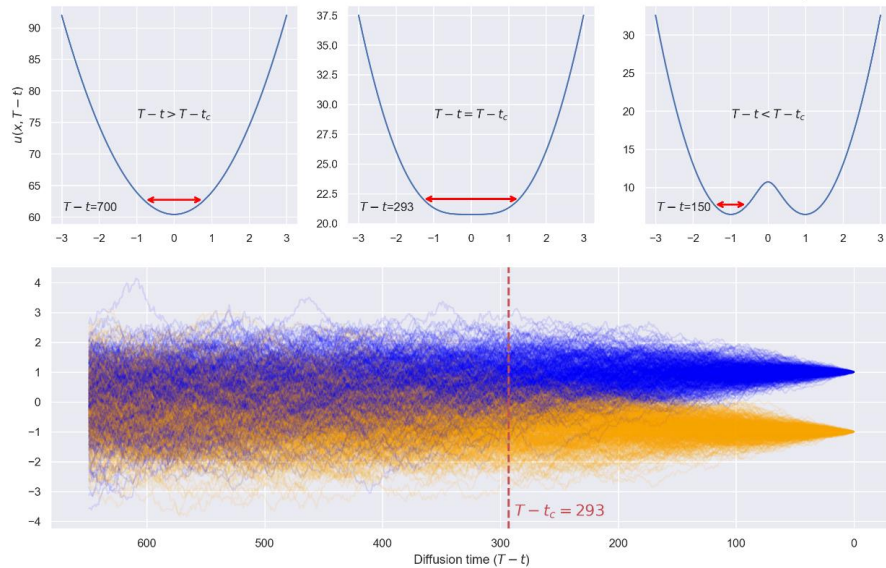
Observation 5. *The (optimal) denoising trajectory converges faster than the (optimal) sampling trajectory in terms of visual quality.*

Figure 5: The synthesized images of our proposed ODE-Jump sampling (bottom) converge much faster than that of EDMs [KAAL22] (top) in terms of visual quality.

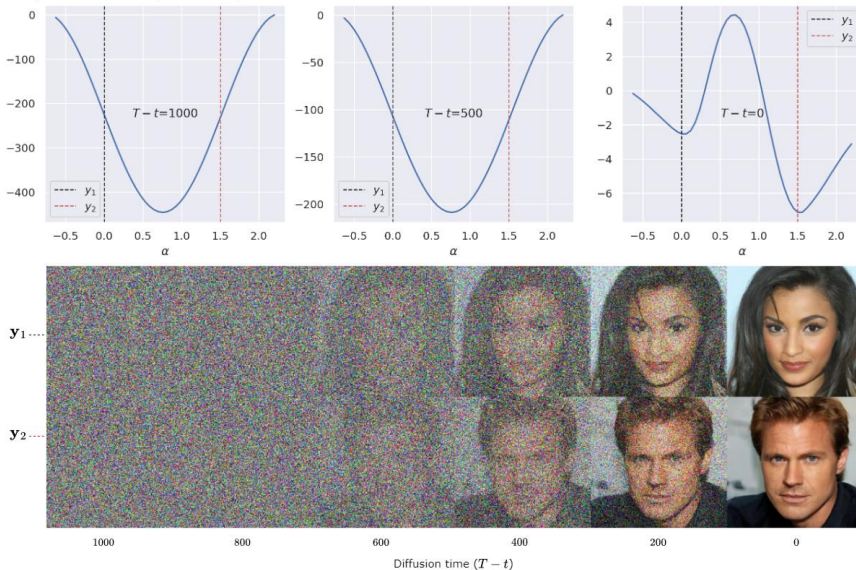
“In fact, our learned score has to moderately diverge from the optimum to guarantee the generative ability.”

Spontaneous symmetry breaking in generative diffusion models*

$$d\mathbf{X}_t = -\nabla_{\mathbf{x}} u(\mathbf{X}_t, T-t)dt + g(T-t)d\mathbf{W}_t$$



(a) Symmetry breaking in 1D diffusion model



(b) Symmetry breaking in CelebA HQ 256x256

$$u(\mathbf{x}, s) = -g^2(s) \log p(\mathbf{x}, s) + \int_0^{\mathbf{x}} f(\mathbf{z}, s) \cdot d\mathbf{z}$$

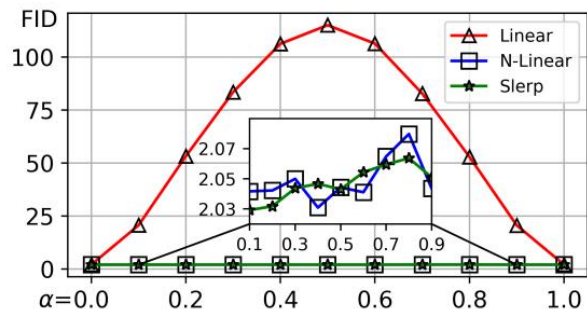
$$u(x, t) = \beta(T-t) \left(-\frac{1}{4}x^2 - \log \left(e^{-\frac{(x-\theta_{T-t})^2}{2(1-\theta_{T-t}^2)}} + e^{-\frac{(x+\theta_{T-t})^2}{2(1-\theta_{T-t}^2)}} \right) \right)$$

*[2305.19693] Spontaneous symmetry breaking in generative diffusion models (arxiv.org)

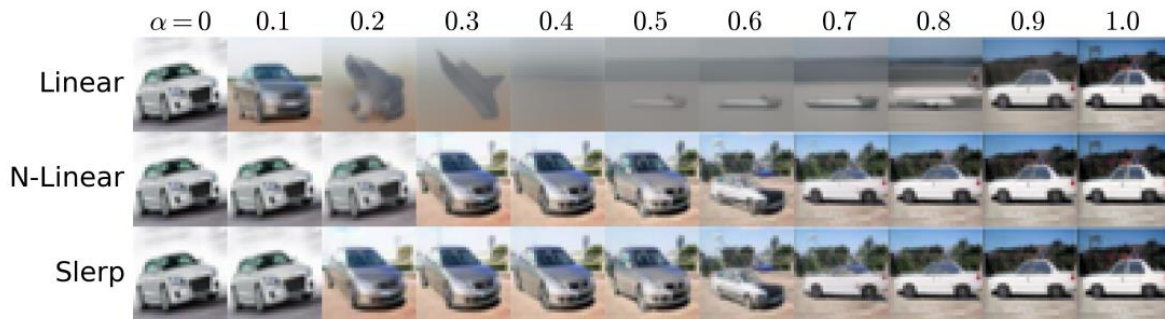
Gabriel Raya | Spontaneous symmetry breaking in generative diffusion models

In-Distribution Latent Interpolation

Proposition 5. *In high dimensions, linear interpolation [HJA20] shifts the latent distribution while spherical linear interpolation [SME21] asymptotically ($d \rightarrow \infty$) maintains the latent distribution.*



(a) The comparison of FID.



(b) Visualization of latent interpolation with different strategies.

Figure 6: Linear latent interpolation results in blurry images, while a simple re-scaling trick greatly preserves the fine-grained image details and enables a smooth traversal among different modes.

Rethinking Distillation-Based Fast Sampling Techniques

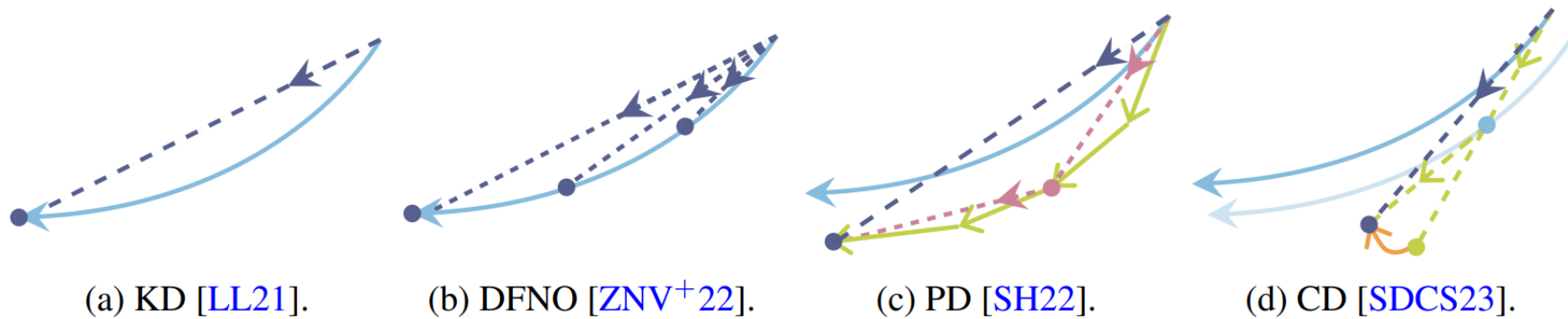


Figure 7: The comparison of distillation-based techniques. The *offline* techniques first simulate a long ODE trajectory with the teacher score and then make the student score points to the final point (KD [LL21]) or also include intermediate points on the trajectory (DFNO [ZNV⁺22]). The *online* techniques iteratively fine-tune the student prediction to align with the target simulated by a few-step teacher model along the sampling trajectory (PD [SH22]) or the denoising trajectory (CD [SDCS23]).

Content

- Motivation
- Geometric Perspective
- Conclusion

Conclusion

- ✓ Geometric perspective on (VE) diffusion models
- ✓ Origin of generative ability
- ✗ Theoretical results do not entirely substantiate the observations
- ✗ Limited to VE-ODE